The Journal of Neuroscience, August 1989, 9(8): 2819–2834

Differential Ascending Projections to Aural Regions in the 60 kHz Contour of the Mustache Bat's Inferior Colliculus

Linda S. Ross[a] and George D. Pollak

Department of Zoology, The University of Texas at Austin, Austin, Texas 78712

The inferior colliculus of the mustache bat is similar in many respects to the inferior colliculus of more commonly studied mammals. However, the isofrequency contour devoted to processing 60 kHz, the dorsoposterior division (DPD) is greatly expanded, encompassing an area approximately equal to one-third of the central nucleus. Of particular significance is that monaural and binaural neurons are segregated in the DPD into 4 spatially distinct aural regions. In this study we exploit the great enlargement of the 60 kHz region in the central nucleus of the inferior colliculus (ICc) of the mustache bat to determine the source of ascending projections to the 4 different aural regions of the DPD. Small iontophoretic deposits of HRP were made within each of the physiologically defined aural regions, and the locations and numbers of retrogradely labeled cells in the auditory brain-stem nuclei were determined. Two major features of collicular organization were found. The first is that each aural region receives a unique set of projections from a subset of lower auditory nuclei and thus is distinguished both by its neural response properties and by the pattern of ascending projections it receives. The dorsomedial EE region receives inputs primarily from the ipsilateral intermediate nucleus of the lateral lemniscus (INLL) and ventral nucleus of the lateral lemniscus (VNLL), and the contralateral ICc. In contrast, the ventrolateral EE region receives projections from the ipsilateral medial superior olivary nucleus (MSO), VNLL, and INLL. The inputs to the EI region originate primarily from the dorsal nucleus of the lateral lemniscus (DNLL) and lateral superior olivary nucleus (LSO) bilaterally and from the ipsilateral INLL. The afferents to the EO region include the contralateral cochlear nucleus, the ipsilateral VNLL and INLL and MSO. The second major organizational feature is that the binaural nuclei of the brain-stem project upon the DPD in a more restricted manner than do some of the lower monaural nuclei, such as the VNLL and INLL, which project in a more widespread manner. The unique set of projections terminating in each aural region of the DPD suggests that the neurons should have substantially different properties, even when neurons in different regions are of the same general aural type. Moreover, the elucidation of the micro-organization of the DPD provides insights into the different ways that binaural properties of DPD neurons are created by the convergence of inputs from particular subsets of lower auditory nuclei. Finally, we point out that the functional organization of the DPD, as revealed in these studies, can be used as a general model for understanding the organization of collicular isofrequency contours.

One of the salient features of the auditory system is the complexity of its subcortical pathways and connections. The pathway ascending between the sensory receptors and the central nucleus of the inferior colliculus (ICc) has at least 3 different synaptic levels: the cochlear nucleus, the superior olivary complex, and the nuclei of the lateral lemniscus. These auditory nuclei appear to serve both relay and integration functions as, at each level of processing, the nuclei are interconnected in a complex series-parallel arrangement with some nuclei projecting to the next level and others passing on to an even higher level.

Despite this complexity, some organizational features are common to nearly all auditory nuclei. First, the ascending projections of the brain-stem auditory nuclei share at least one common target, the ICc (van Noort, 1969; Roth et al., 1978; Adams, 1979; Brunso-Bechtold et al., 1981; Schweizer, 1981; Warr, 1982; Zook and Casseday, 1982b; Aitkin, 1985). Second, each nucleus contains an orderly representation of frequency information and thus a single tonotopic arrangement (Rose et al., 1959; Tsuchitani and Boudreau, 1966; Goldberg and Brown, 1968; Guinan et al., 1972b; Aitkin, 1976; Irvine, 1986).

The ICc also has a single tonotopic map, which in most mammals takes the form of a series of dorsoventrally ordered isofrequency contours (Merzenich and Reid, 1974; FitzPatrick, 1975; Aitkin, 1985; Pollak and Casseday, 1989). This single map of frequency is remarkable when one considers that separate projections from 10 or more lower brain-stem nuclei converge upon the ICc and that each of the contributing nuclei is itself tonotopically organized. Apparently as the multiple tonotopic maps converge upon the ICc they are sorted in an orderly manner to reconstitute the single tonotopic map within the ICc.

The massive convergence at the level of the ICc also suggests that the projections are sorted by function, as well as by frequency, with the isofrequency contour acting as the organizational unit. Consistent with this are previous physiological studies of the cat's ICc showing that binaural response properties are grouped within isofrequency contours (Roth et al., 1978; Semple and Aitkin, 1979). Furthermore, the projections of lower brain-stem nuclei terminate regionally upon the ICc in a manner

Received Oct. 31, 1988; revised Jan. 16, 1989; accepted Jan. 19, 1989.

We thank J. Zook, J. Winer, J. Wenstrup, H. Zakon, W. Thompson, J. Larimer, Z. Fuzessery, D. Ryugo, and W. Wilczinski for their helpful comments and suggestions. We also thank Carl Resler for technical assistance and Janet Young for artwork. This work supported by PHS grant NS13276 (G.D.P.) and a University Fellowship awarded to L.S.R.

Correspondence should be addressed to Dr. George D. Pollak at the above address.

[a] Present address: Department of Biology, University of Michigan, Ann Arbor, MI 48109.

consistent with the grouping of physiological response properties within an isofrequency contour (Roth et al., 1978; Brunso-Bechtold et al., 1981; Aitkin and Schuck, 1985; Maffi and Aitkin, 1987). However, the internal organization of isofrequency contours has been difficult to study because in most mammals the contours are narrow and sharply curved. These physical limitations have prevented investigators from directly correlating the topography of response properties along a contour with any regional distribution of inputs from lower centers. For reasons given below, these limitations are not present in the mustache bat's ICc, which serves as a model system to examine aspects of the micro-organization of an isofrequency contour.

The organization of the inferior colliculus (IC) of the mustache bat is consistent with the patterns seen in other mammals (Zook et al., 1985; Wenstrup et al., 1986). Similar cell types are present and there is a single tonotopic organization. The isofrequency contour devoted to processing 60 kHz, however, is greatly expanded (Pollak and Bodenhamer, 1981; Pollak et al., 1983; Zook et al., 1985) and encompasses an area approximately equal to one-third of the central nucleus, which has been named the dorsoposterior division (DPD). The DPD forms a large wedge-shaped region between the other 2 divisions of the ICc, the medial division (MD), and the anterolateral division (ALD) (Pollak et al., 1983; Zook et al., 1985). Both the MD and ALD contain the pronounced fibrodendritic laminae that, in other mammals, are the presumptive anatomical substrates of isofrequency contours observed physiologically (Rockel and Jones, 1973; Merzenich and Reid, 1974; Oliver and Morest, 1984; Serviere et al., 1984). Physiological recordings show that the ALD contains an orderly representation of frequencies from 10–60 kHz along the rostrocaudal dimension, and the MD contains an orderly representation of high frequencies from about 64–120 kHz. The DPD has many of the same cell types found within the fibrodendritic laminae of other frequency representations of the ICc. In contrast to the ALD and MD, the DPD is characterized physiologically by the frequency uniformity of its neuronal population, where all neurons are sharply tuned to 60 kHz and have best frequencies that differ by only about ±300 Hz among the population (Pollak et al., 1983; Zook et al., 1985). Although the DPD is of unusual proportions, it represents a single elaborated isofrequency contour as defined by anatomical and physiological criteria.

In a previous study we showed that the DPD receives ascending projections from all lower auditory nuclei (Ross et al., 1988). The projections emanate from the contralateral cochlear nucleus and ICc, from the ipsilateral medial superior olivary nucleus (MSO), ventral nucleus of the lateral lemniscus (VNLL), and intermediate nucleus of the lateral lemniscus (INLL), and from the lateral superior olivary nucleus (LSO) and dorsal nucleus of the lateral lemniscus (DNLL) bilaterally. Furthermore, the projections to the DPD arise from discrete segments of the various projecting nuclei, each of which presumably represents 60 kHz. DPD neurons possess a wide variety of aural response properties, in agreement with the diversity of inputs from nuclei that have monaural or binaural response properties (Fuzessery and Pollak, 1985; Wenstrup et al., 1986). In addition to monaural neurons, 2 major binaural types are common in the DPD: those receiving excitation from the 2 ears, the EE neurons, and those receiving excitation from one ear and inhibition from the other, the EI neurons. Of particular significance, Wenstrup et al. (1986) observed that monaural and binaural neurons are topographically organized, forming 4 different aural regions within the DPD. For purposes of orientation the locations of these aural regions, as reported by Wenstrup et al., are shown in Figure 1. The monaural neurons are located along the dorsal and lateral parts of the DPD. EE neurons occur in 2 regions: one in the ventrolateral DPD and another in the dorsomedial DPD. The main population of EI neurons is in the ventromedial DPD. We will not consider the EI neurons in the far lateral IC since these are most likely in the external nucleus of the IC.

The presence of a topographic organization of binaural response properties within the DPD, coupled with the reception of a full complement of auditory input, implies that the projections from the various parallel pathways of the brain stem terminate within the DPD in a segregated manner. A segregated projection pattern would preserve the functionally distinct properties of the lower nuclei as they converge on their common substrate, the ICc.

In this study, we exploit the great enlargement of the 60 kHz region in the mustache bat's ICc to determine the source of ascending projections to the 4 different aural regions of the DPD. Here, we report the results from making small iontophoretic deposits of HRP within each of the physiologically defined aural regions and noting the locations and numbers of retrogradely labeled cells in the auditory brain-stem nuclei.

Materials and Methods

Surgical procedures. Thirty mustache bats (*Pteronotus parnellii*) were used in these experiments. Prior to surgery, animals were anesthetized with methoxyflurane inhalation (Metofane, Pitman-Moore, Inc.) and an intraperitoneal injection of sodium pentobarbital (Nembutal, Abbott Laboratories) at a dosage of 10 mg/kg. The animal's head was secured in a head holder with a bite bar. The muscles and skin overlying the skull were reflected laterally, and lidocaine (Elkins-Sinn, Inc.) was applied topically to the open wounds. The surface of the skull was cleared of tissue, and a layer of small glass beads and dental acrylic was placed on the surface. A hole was drilled over the IC using landmarks visible through the skull for orientation.

The bat was transferred to a heated recording chamber, where it was placed in a Plexiglas restraining apparatus. A metal pin was cemented to the foundation layer on the skull and then attached to the restraining apparatus to ensure a uniform positioning of the head for mapping experiments. A ground electrode was placed between the previously reflected muscles and skin. Recordings were begun after the bat was awake since the thresholds of neurons tuned to 60 kHz in this species are greatly increased by general anesthetics. Supplemental doses of Acepromazine (2 mg/kg; acepromazine maleate, Aveco Co., Inc.) and Nembutal (5 mg/kg) were given for sedation. Lidocaine was regularly applied to the scalp incision throughout the recording session.

Acoustic stimulation. Sine waves were generated with a Wavetek function generator (model 136) and monitored with a frequency counter. The sine waves were fed to a custom-made electronic switch to shape tone bursts that were 30 msec in duration, had 1 msec rise/fall times, and were presented at a rate of 3–4 bursts/sec. The electronic switch had 2 independent outputs that were fed to 2 attenuators (Hewlett-Packard, model 350D). The outputs of the attenuators were connected to 2 Polaroid condensor speakers (model T2004), each biased with 200 VDC. Each speaker was fitted with a funnel ending in a tube diameter of 5 mm that was fitted into one of the ears, next to the external meatus, and sealed in place with ear mold compound. This was the same arrangement used in previous studies (Wenstrup et al., 1986; Ross et al., 1988) and created an acoustic isolation of at least 40 dB between the 2 ears.

Recording procedures. Dorsoventral penetrations through the DPD were made at an angle of approximately 7° from vertical. The surface vasculature served as landmarks for placement of the recording electrode, and the penetration sites were recorded on a drawing of the collicular surface. Multiunit responses were recorded with glass micropipettes mechanically blunted to a tip diameter of 5–10 μm. Electrodes were filled with a 30% solution of HRP (Sigma, Type VI) in 1 M NaCl (pH 7.6), previously filtered with centrifuge microfilters (Schleicher & Schuell). Electrodes were lowered with a Kopf hydraulic system con-

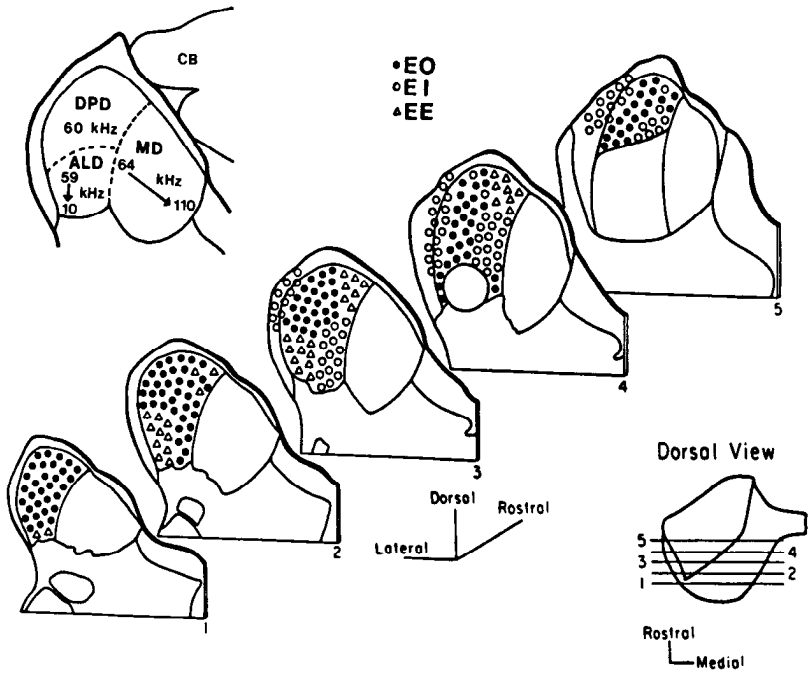

Figure 1. Schematic illustration of the segregation of binaural response properties in the dorsoposterior division (DPD) of the mustache bat's IC. In the *center* are transverse sections of the IC arranged in a caudal to rostral manner. Each section is separated by 180 μm. The *lower-right* panel shows the rostrocaudal position of each section illustrated on the dorsal view of the IC. The smaller *outlined* area shows the portion of the IC that is not covered by the cerebellum and thus was visible. The *larger* area shows the full outline of the IC when the cerebellum is removed. In the *upper-left* panel, the medial division (MD), where high frequencies are represented, and the anterolateral division (ALD), representing frequencies below 60 kHz, are labeled. This section is representative of the IC at a rostrocaudal location midway between sections 4 and 5 shown below. Symbols (EO neurons, ●; EE neurons, △; EI neurons, ○) indicate binaural properties of unit clusters recorded in DPD and adjacent external nucleus of the IC. Figure adapted from Wenstrup et al. (1986).

trolled by a stepping motor outside the experimental chamber. Neural responses were amplified and band-pass-filtered by conventional methods and displayed audiovisually. The output of the amplifier was also sent through a window discriminator (Frederick Haer & Co.) and then to a Declab 11/03 computer that generated poststimulus time (PST) histograms and spike counts.

The multiunit responses consisted of stimulus-locked clusters of clearly defined spikes that varied in amplitude and shape. At each recording site, the best frequency (BF), the frequency to which the neuronal cluster was most sensitive, and the threshold at BF were determined audiovisually. The binaural property of the cluster was then determined. The contralateral intensity was set at 15 dB above threshold, and the effect of simultaneous ipsilateral stimulation was determined from 30 dB above to 30 dB below the intensity at the contralateral ear. The effects of binaural stimulation were assessed both audiovisually and with PST histograms that also provided spike counts. When generating PST histograms, the window discriminator was set to detect spike activity exceeding the baseline noise activity. Large, medium, and some smaller amplitude spikes were thereby included in the generation of the histograms of spike trains. The responses of neuron clusters in the DPD were divided into 3 general classes based on their responses to dichotic stimulation (Fig. 2). EO or monaural responses displayed an excitatory response only to sounds presented to the contralateral ear and were unaffected by sounds at the ipsilateral ear presented either alone or simultaneously with the contralateral sound. Responses were classified as EE when an excitatory response was evoked by monaural presentation of both ipsi- and contralateral sound. Responses were classified as EI when discharges were evoked by contralateral sound but were not evoked by ipsilateral sounds, and when the discharges elicited by contralateral sounds were inhibited by the simultaneous presentation of sound at the ipsilateral ear. The maximum interaural intensity disparity generated by the mustache bat's external ears at 60 kHz is about 30 dB (Fuzessery and Pollak, 1985). Thus, a neuron was considered binaural only if ipsilateral sound produced an excitatory or inhibitory effect when the intensity was within 30 dB of the intensity at the contralateral ear.

Multiunit responses were monitored every 75–100 μm along a penetration. At each locus the BF, threshold at BF, and the binaural category of the cluster were evaluated. The electrode was advanced until an abrupt change in BF and tuning sharpness indicated that the electrode had left the DPD. Deposits of HRP were made only when (1) the aural properties recorded along a penetration were clear and well-defined, and (2) there was a clear segregation of the aural responses encountered along the penetration. When these 2 conditions were met, the electrode was then retracted to a position centered within an aural response region. Additional PST histograms were collected to corroborate the binaural category at that location, and subsequently a focal deposit of HRP was made by passing 1.5–1.8 μA of positive pulsed current for a period of 30–40 min. The sizes of the deposit sites were small, typically ranging from about 75–150 μm (Fig. 2). The use of 30% HRP in the electrodes enhanced the amount of the enzyme at the deposit site and thereby also enhanced the amount of retrograde transport. In 4 animals, a second deposit was made along the penetration at a site with similar binaural response properties to increase the likelihood of sufficient retrograde transport of HRP.

Histological procedures. Following a survival period of 24–36 hr, the bats were deeply anesthetized with methoxyflurane and then perfused intracardially with a PBS solution followed by a 4% glutaraldehyde solution at room temperature. The brains were blocked in the same plane as the electrode penetrations, and then refrigerated 6–8 hr in a 30% sucrose–PBS. Transverse sections were cut at 30 μm on a freezing microtome, and alternate sections were reacted with TMB (Mesulam, 1982) or DAB (Adams, 1981), and then counterstained lightly with either neutral red, safranin O (TMB), or with cresyl violet (DAB).

Data analysis. All auditory nuclei were examined at magnifications of 100–400× for the presence of labeled cell bodies using both bright- and dark-field illumination. The locations of labeled cells were plotted onto outline drawings of the brain-stem sections made with a drawing tube. The cytoarchitectural criteria of Zook and Casseday (1982a) for defining auditory brain-stem nuclei were used to assign the nomenclature and boundaries of architectonic subdivisions. The criteria are based on cell size, shape, and dendritic orientation.

The number of labeled cells in each auditory nucleus was counted in each case, using the TMB-reacted sections. In 3 cases, the label in the TMB cases faded after staining and so cells were counted in these cases using the DAB-reacted sections. The cell counts were then converted to a percentage by dividing the number of labeled cells in a given auditory nucleus by the total number of labeled cells found in that case, and then multiplying by 100. The data from all cases of an aural region were combined to calculate the average percentage for each nucleus that was found to project to an aural region. Nonauditory nuclei and regions rostral to the ICc were not sampled for the presence of retrogradely labeled cells.

Deposit sites were reconstructed by measuring the coordinates of the deposit site within the ICc in the following manner. First, the transverse section in which the deposit site was centered was determined, and an outline drawing of this section was made. Mediolateral coordinates were measured as the distance from the midline of the section to the center of the deposit site. The vertical distance from the collicular surface to the center of the deposit site represented the dorsoventral coordinate. The position of the deposit site along the rostrocaudal axis was deter-

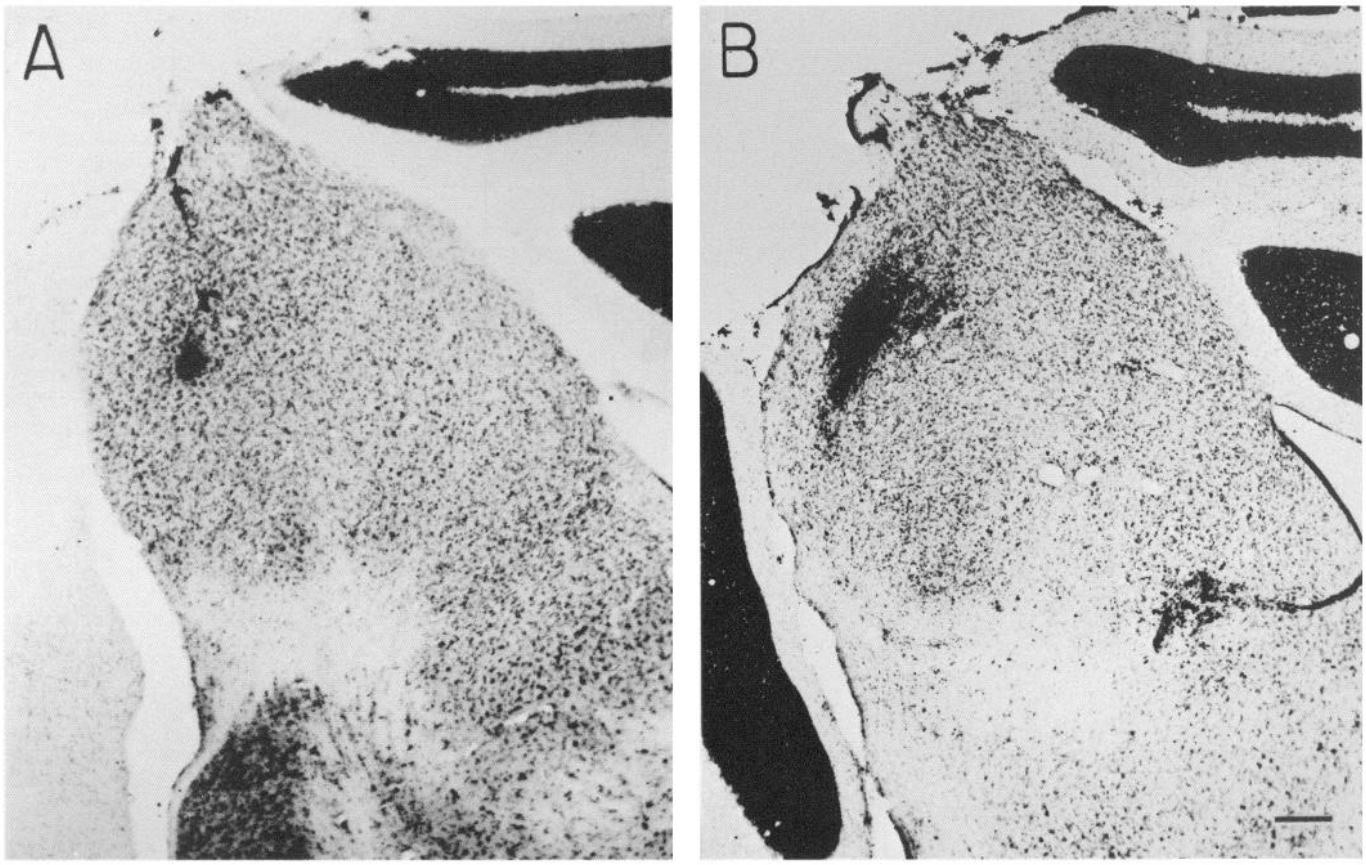

Figure 2. Transverse sections of the IC from 2 bats illustrating the range of sizes of the HRP deposits in this study. The sections were reacted with DAB and counterstained with cresyl violet. *A*, Case P7-29-87 that had the smallest deposit site of any of the bats used in this study. Twenty-five labeled cells, resulting from this deposit, were found in the brain-stem auditory nuclei. *B*, Case P7-30-87, which illustrates a larger deposit than in *A*. Ninety-two labeled cells were found in the auditory brain-stem nuclei in this case. Scale bar, 200 μm.

mined by counting the number of sections from the caudal pole of the IC to the deposit site. This distance was also converted to a percentage of the rostrocaudal axis of the IC by dividing the rostrocaudal position of the deposit site by the total rostrocaudal length of the ICc. Using the 3-dimensional coordinates, the location of the deposit site was plotted onto a set of standardized drawings of transverse IC sections as shown in Figure 4; the coordinates of the aural regions are summarized in Table 1.

Results

Deposit site locations

Neurons having the same aural properties were typically encountered along extended segments of dorsoventral electrode penetrations through the DPD. In Figure 3 there are drawings of transverse sections through the DPD from 3 bats. In each section, the distribution of binaural and monaural neurons found along the electrode tracts are indicated, together with the loci of HRP deposits. For each case, the aural properties of the neurons at the HRP deposit site were confirmed by PST histograms of the responses evoked by monaural and binaural stimulation to the ipsi- and contralateral ears. The top panel shows an electrode tract where monaural neurons were primarily encountered. The middle panel illustrates a case in which an HRP deposit was made along a tract where EE neurons were the predominant type, and the lower panel shows a tract where EI neurons were recorded.

Figure 4 illustrates the location of all deposit sites reconstructed in this study, distinguished in terms of the binaural response characteristics of the region in which the deposit was made. The coordinates of all deposit sites, classified by binaural response properties, are summarized in Table 1. Four aural regions were identified having locations similar to those found previously by Wenstrup et al. (1986) (see Fig. 1). A large monaural EO region lies dorsally and extends through most of the rostrocaudal extent of the DPD (Fig. 4, sections 1–5). In caudal portions of the DPD (Fig. 4, sections 2 and 3), a region of binaural EE neurons lies ventrolaterally, beneath the dorsal layer of EO neurons. This region of EE neurons is distinct from a separate EE region located dorsally and somewhat more medially in the far rostral portions of the DPD (Fig. 4, sections 3 and 4). The fourth aural region of the DPD, the EI region, was

Table 1. Distribution of deposit sites within aural regions of the DPD

	Site (μm)		
Response type	D-V	M-L	R-C
Dorsomedial EE (4 cases)	250–710	1240–1690	810–1270
Ventolateral EE (4 cases)	550–870	1450–2120	560–1020
EI (2 cases)	260–1060	1200–1540	640–800
EO (8 cases)	160–870	1660–2310	240–1560

For deposits in each aural region, the range of the coordinates in the dorsoventral (D-V), mediolateral (M-L) and rostrocaudal (R-C) planes of the IC are shown.

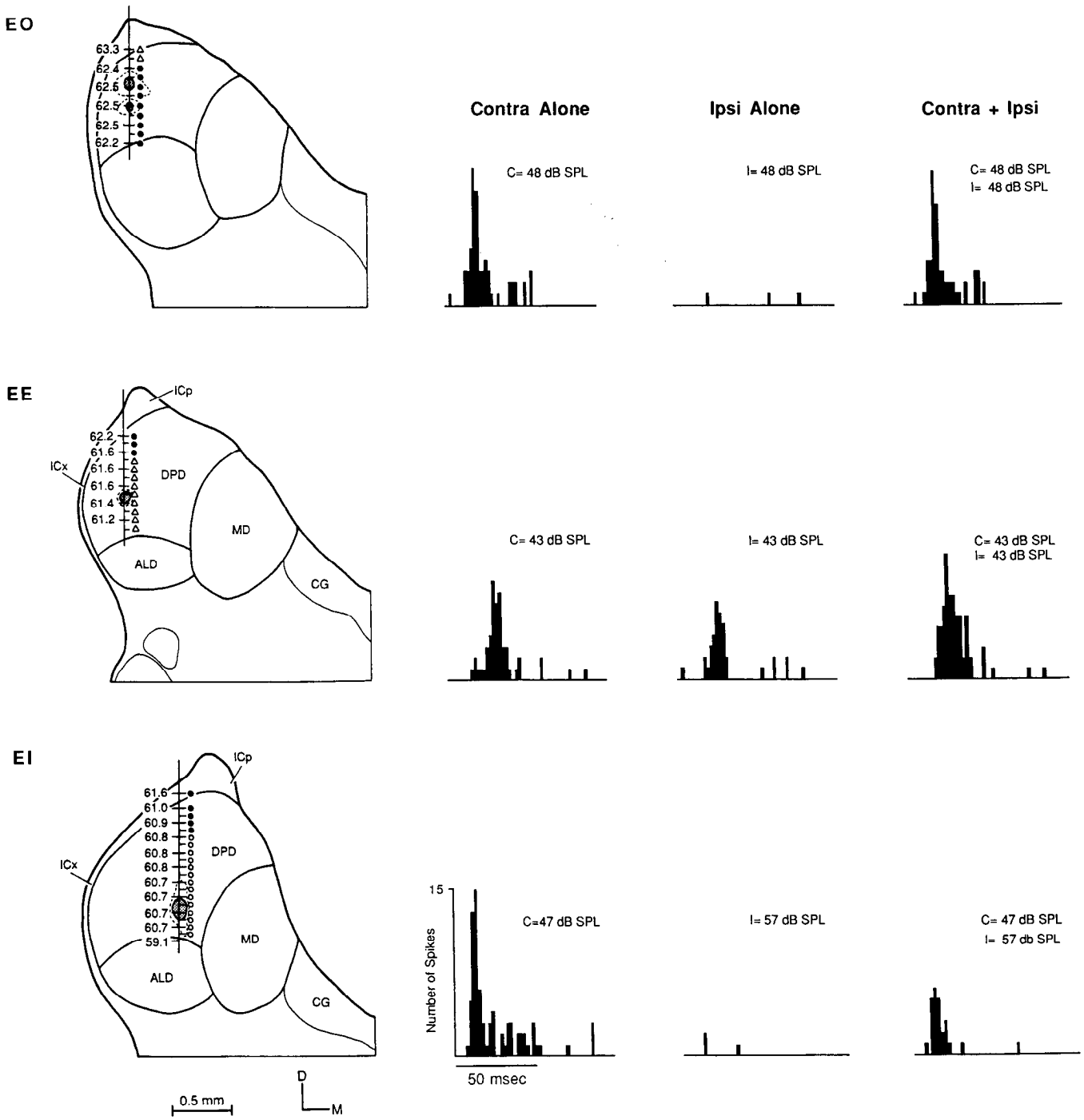

Figure 3. Transverse sections through the DPD from 3 bats. In each section, the best frequency and aural category of the unit clusters recorded along the electrode tracts are indicated, together with the loci of HRP deposits. The best frequencies are shown at the *left* of the electrode tract and the aural response properties at the *right*. The deposit sites are indicated by the *stippled circle* and the spread of extracellular reaction product is indicated by the *dashed line*. For each case, the aural properties of the neurons at the HRP deposit site are documented with PST histograms of the responses evoked by monaural stimulation to the ipsilateral and contralateral ears, and with binaural stimulation. Symbols: EO neurons, ●; EI neurons, O; EE neurons, △.

located caudally in ventromedial portions of the DPD (Fig. 4, section 3).

Small iontophoretic deposits of HRP assured that the deposit would be confined to the immediate vicinity of the recording site. Twenty of the 30 cases illustrated in Figure 3 contained retrogradely labeled cells in the brain-stem auditory nuclei. In these cases, the labeled cells were restricted to regions of the lower auditory nuclei that were previously identified as representing 60 kHz (Ross et al., 1988). In any one case, however, only a small set of auditory nuclei contained the majority of the labeled cells, and the specific set of auditory nuclei that were labeled varied as a function of the aural response characteristics

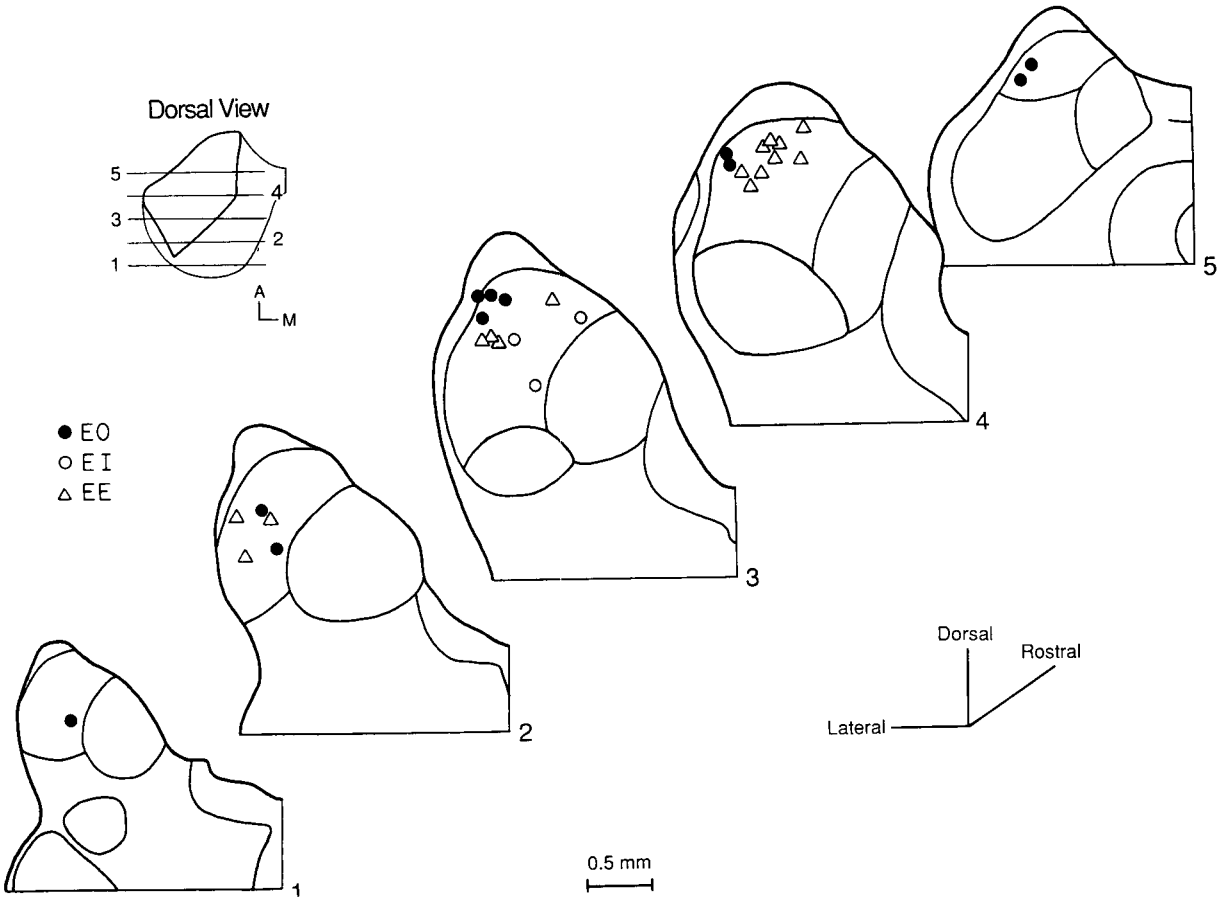

Figure 4. Schematic illustration showing the location and aural response properties at HRP deposit sites reconstructed in this study. Transverse sections of the IC are separated by 320 μm along the rostrocaudal axis of the IC. *Upper left,* Dorsal view of the IC illustrating the location of sections 1–5 along the rostrocaudal axis. Symbols: EO neurons, ●; EI neurons, ○; EE neurons, △.

of the deposit site. Two of the 20 cases containing retrogradely labeled cells were excluded from further analysis because the HRP spread into adjacent aural regions.

The afferents to each of the aural regions are described below. The nuclei that provide the major input to each aural region are identified, and the proportion of labeled cells in each nucleus is illustrated by the histograms from representative cases. This pattern of labeling is compared with the sparse labeling or absence of labeling in other auditory nuclei.

Inputs to dorsomedial EE region

The projections to the dorsomedial EE region arise chiefly from 3 nuclei: the contralateral ICc, and the ipsilateral VNLL and INLL. Figure 5 graphs the distribution of labeled cells from 2 cases in which deposits were made within the dorsomedial EE region. Based on 4 cases, the contralateral ICc contained 33% of the total number of labeled cells, the VNLL had 27%, and the INLL had 19%. These 3 nuclei were the primary contributors in all 4 cases with deposits in this EE region. In 3 of 4 cases, the contralateral ICc contained the most labeled cells. The VNLL and INLL contained significant numbers of labeled cells, although less than in the contralateral ICc. In 1 case (not shown), the contribution from the ipsilateral VNLL exceeded that of the contralateral ICc. Also not shown were small projections (<5%) bilaterally from the lateral nucleus of the trapezoid body (LNTB) and ipsilaterally from the anterolateral periolivary nucleus (ALPO), dorsomedial periolivary nucleus (DMPO), and ventromedial periolivary nucleus (VMPO) in all 4 cases.

Labeled cells in the contralateral ICc were located primarily in the dorsomedial DPD in each case at a site symmetrical to the deposit (Fig. 6). Besides the labeled cells in the contralateral ICc, labeled fibers and terminals were also seen (top, Fig. 6). The presence of both fibers and retrogradely labeled cells suggests that the dorsomedial EE region has reciprocal connections with the same region in the contralateral DPD. In these cases, labeled terminals and fibers were also consistently observed in 2 other locations, the nucleus of the brachium of the inferior colliculus (nBIC) and in more ventrolateral portions of the caudal DPD.

Figure 5 also shows that several nuclei provided either sparse projections to the dorsomedial EE region or no projections at all. The 3 divisions of the cochlear nucleus projected inconsistently to this binaural region with each division contributing an average of less than 2% of the total number of labeled cells. Particularly striking is the near absence of projections from binaural nuclei, such as the LSO, MSO, and DNLL. When the data from all 4 cases with medial EE deposits are combined, the average percentage of labeled cells in each of these nuclei was less than 4% of the total. The near absence of labeled cells in the LSO, MSO, and DNLL is conspicuous in these cases since these nuclei project heavily to other aural regions of the DPD (see below).

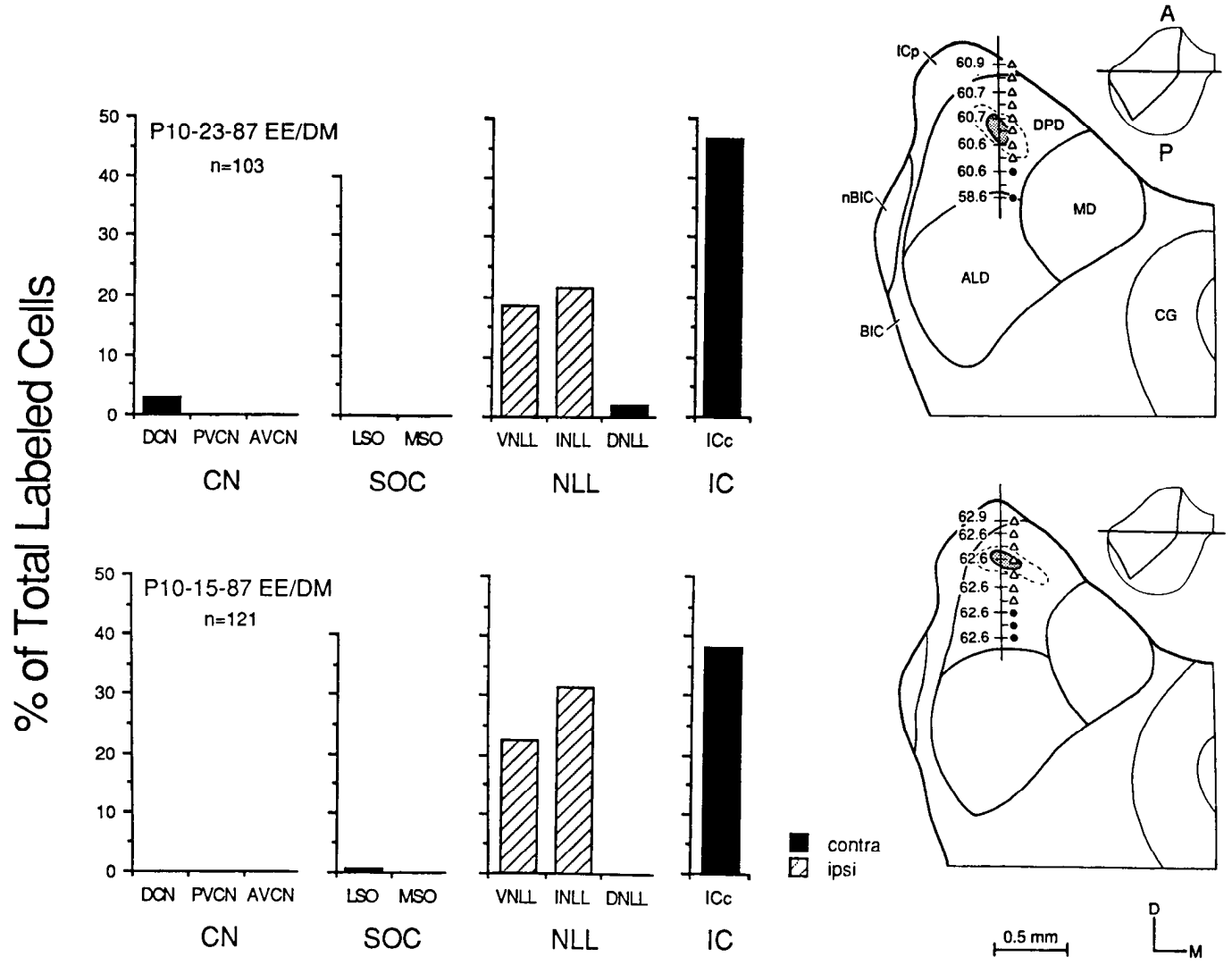

Figure 5. *Left*: Bar graphs illustrating the distribution of labeled cells following deposits of HRP in the dorsomedial EE region in 2 representative cases. The percentage of labeled cells found in each nucleus is shown, with *striped bars* indicating cells in the ipsilateral nuclei and *black bars* indicating cells in the contralateral nuclei. *Right,* Reconstructions of electrode tracts and deposit sites. *Stippled circles* indicate the extent of the deposit site and the *dashed line* represents the spread of extracellular reaction product. Best frequency at each locus is indicated at the *left* and aural response property at the *right* of the tick marks along the electrode tracts. A dorsal view of the IC is shown in the *upper right* to illustrate the location of the section along the rostrocaudal axis of the IC. Note that the largest percentages of labeled cells were found in the ipsilateral INLL, VNLL, and the contralateral ICc. Symbols: EO neurons, ●; EE neurons, △.

Inputs to ventrolateral EE region

The primary input to the ventrolateral EE region originates in the ipsilateral MSO, VNLL, and INLL. The distribution of labeled cells following 2 deposits in this region are shown in Figure 7. On average, the percentage of labeled cells in these nuclei were as follows: MSO, 25%; VNLL, 28%; and INLL, 12%. These 3 nuclei were the major contributors in 3 of 4 cases with deposits in the ventrolateral EE region, and the VNLL contained the highest percentage of labeled cells in 3 cases. The fourth case (not illustrated) involved a deposit at the extreme lateral border of the DPD and consequently displayed a somewhat different distribution of labeled cells. In this lateral case, the ipsilateral MSO contained the highest number of labeled cells (42%), and there were more labeled cells located in the contralateral anteroventral cochlear nucleus (AVCN) (18%) than in the ipsilateral VNLL (12%) or INLL (5%). This difference probably reflects the regional distribution of projections from the MSO and AVCN, as discussed in a later section.

The AVCN consistently contained labeled cells, although in 3 of the 4 cases it contained less than 7% of the total number of labeled cells. The contralateral posteroventral cochlear nucleus (PVCN) contained labeled cells in 3 of the 4 cases with an average of 4%. The only periolivary nucleus that consistently contained labeled cells was the ipsilateral VMPO. This nucleus contained sparse labeling in 3 of 4 cases.

Several nuclei showed no evidence of projecting to the ventrolateral EE region or sent only sparse afferents to this region. While the ICc was the main contributor to the dorsomedial EE region, the ICc showed no evidence of projecting to the ventrolateral EE region in 2 cases (Fig. 7) and very sparse projections in 2 other cases (representing only 8 and 3% of the total). Although the DNLL had 17% of the labeled cells in 1 case (P9-

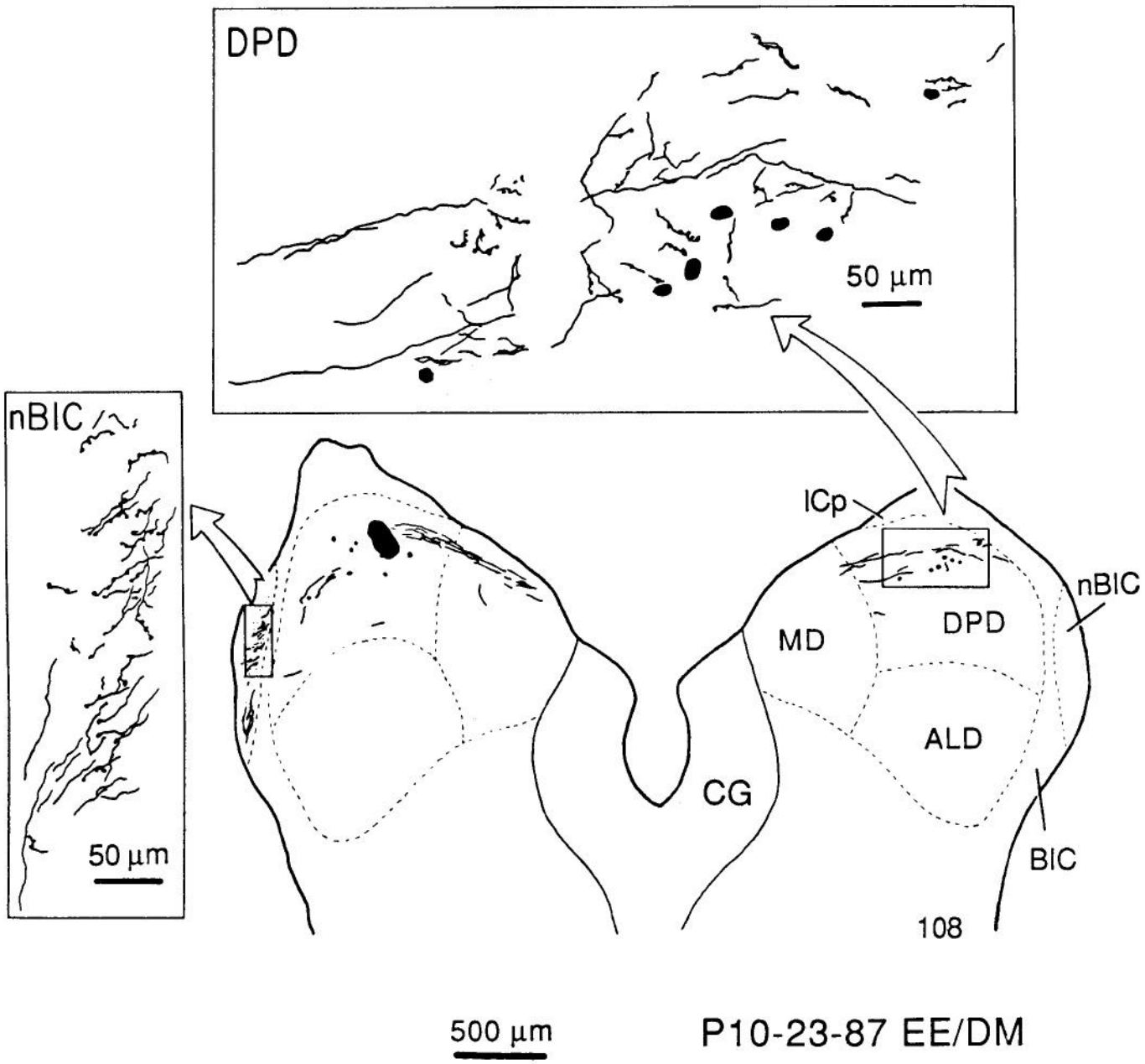

Figure 6. Drawing of HRP-filled fibers and terminals from a deposit in the dorsomedial EE region of the DPD. A transverse section of the IC shows the presence of labeled fibers and terminals in a site symmetrical to the deposit site in the contralateral DPD (*upper right*), and in the ipsilateral nucleus of the brachium of the inferior colliculus (nBIC) on the *left*. Labeled cell bodies are indicated by *black dots*.

15-87A of Fig. 7), in other cases the DNLL contained only sparse labeling, having an average of less than 7%.

Projections to the EI region

Following deposits in the EI region, labeled cells were primarily located in the ipsilateral INLL and bilaterally in the DNLL. Smaller numbers of labeled cells were found in both the contra- and ipsilateral LSO. The distribution of labeled cells following HRP deposits in the EI region in 2 cases are illustrated in Figure 8. In these cases, the INLL, DNLL, and LSO contained 29, 36, and 12% of the labeled cells, respectively. The ventromedial EI region is the only region of the DPD in which even moderate projections from the LSO were consistently observed. Likewise, the DNLL contained only sparse labeling with HRP deposits in other aural regions, but contained large numbers of labeled cells in cases involving deposits in the EI region. A few labeled cells were observed in the contralateral dorsal cochlear nucleus (DCN) (5%) and ICc (7%) in both cases. The ipsilateral LNTB was the only periolivary nucleus that consistently contained labeled cells, but only contained an average of 2% of the total labeled cells.

Labeled cells were noticeably absent from the ipsilateral VNLL and MSO and the contralateral PVCN and AVCN. Case P4-27-86 contained a small amount of labeled cells in these nuclei, but in case P8-23-86, no labeled cells were observed in any of

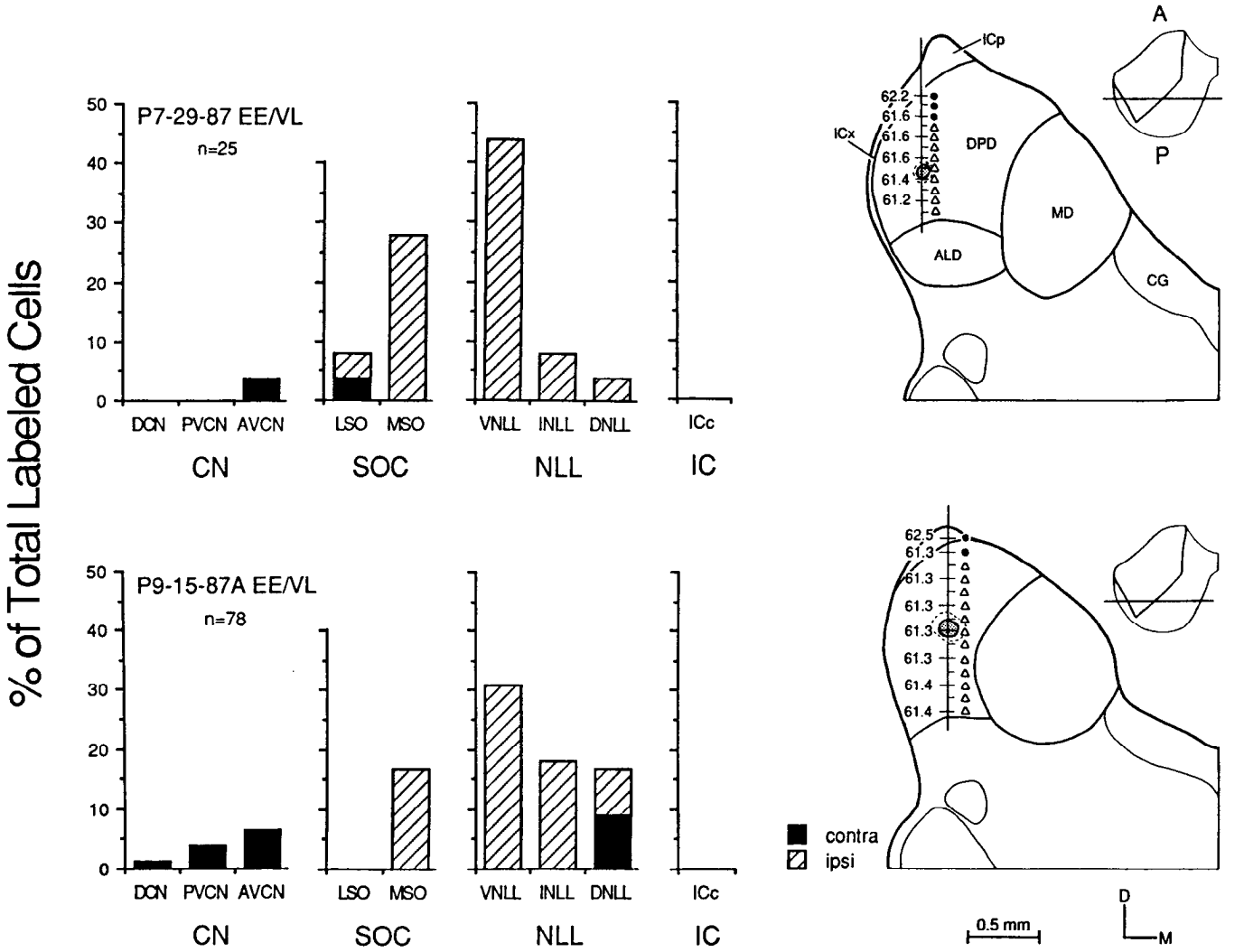

Figure 7. Two cases showing the percentage of labeled cells in the lower auditory nuclei following deposits in the ventrolateral EE region of the DPD (see Fig. 5 for explanation). Note the heavy projections from the ipsilateral VNLL, INLL, and MSO in both cases. The larger percentage of labeled cells located in the DNLL in case P9-15-87A is probably due to the ventromedial location of the deposit site. Symbols: EO neurons, ●; EE neurons, △.

these nuclei. The absence of label in the VNLL and MSO is especially evident, because these 2 nuclei project heavily to other aural regions.

Projections to the EO region

Labeled cells were primarily found in 3 nuclei following deposits in the dorsal EO region: the ipsilateral INLL, VNLL, and MSO (Fig. 9, Table 2). These 3 nuclei were the major sources of projections in 6 of the 8 EO cases. In the exceptions, the projections from the contralateral ICc exceeded those from the MSO in 1 case, and the projections from the cochlear nuclei exceeded the projections from the MSO in the other case. In 8 cases, the INLL had 15% of the total number of labeled cells, the VNLL 37%, and the MSO 18%.

Of the 3 nuclei found to be the primary source of projections, the VNLL usually contained the highest percentage of labeled cells. However, in 3 of the 8 cases, more labeled cells were located in the ipsilateral MSO than in the VNLL. The cochlear nuclei consistently contained labeled cells following EO deposits. Labeled cells were observed in the contralateral AVCN in all 8 cases, and in the PVCN and DCN in 7 of 8 and 6 of 8 cases, respectively. The ipsilateral LNTB and ALPO nearly always contained sparse labeling. The DNLL usually contained labeled cells bilaterally, but never more than 7% of the total. Labeling in the LSO was more variable, occurring in 5 of 8 cases, with no more than 6% of the total labeled cells ever found in any case. Sparse labeling was seen in the contralateral ICc in only 4 of the 8 cases.

The VNLL and INLL contained a large percentage of the labeled cells in all cases, implying that these 2 nuclei project throughout the rostrocaudal extent of the EO region. The MSO, however, appears to project in a differential pattern within the EO region. In caudal portions of the EO region (Fig. 9, case P7-18-85), only small numbers of labeled cells were found in the MSO, while a larger percentage of the labeled cells occurred in monaural nuclei, such as the cochlear nuclei and the VNLL and INLL. When deposits were located midway along the rostrocaudal axis of the ICc (Fig. 9, cases P7-30-87 and P7-27-87), the MSO contained the majority of labeled cells, although labeling in the VNLL and INLL was substantial. In rostral por-

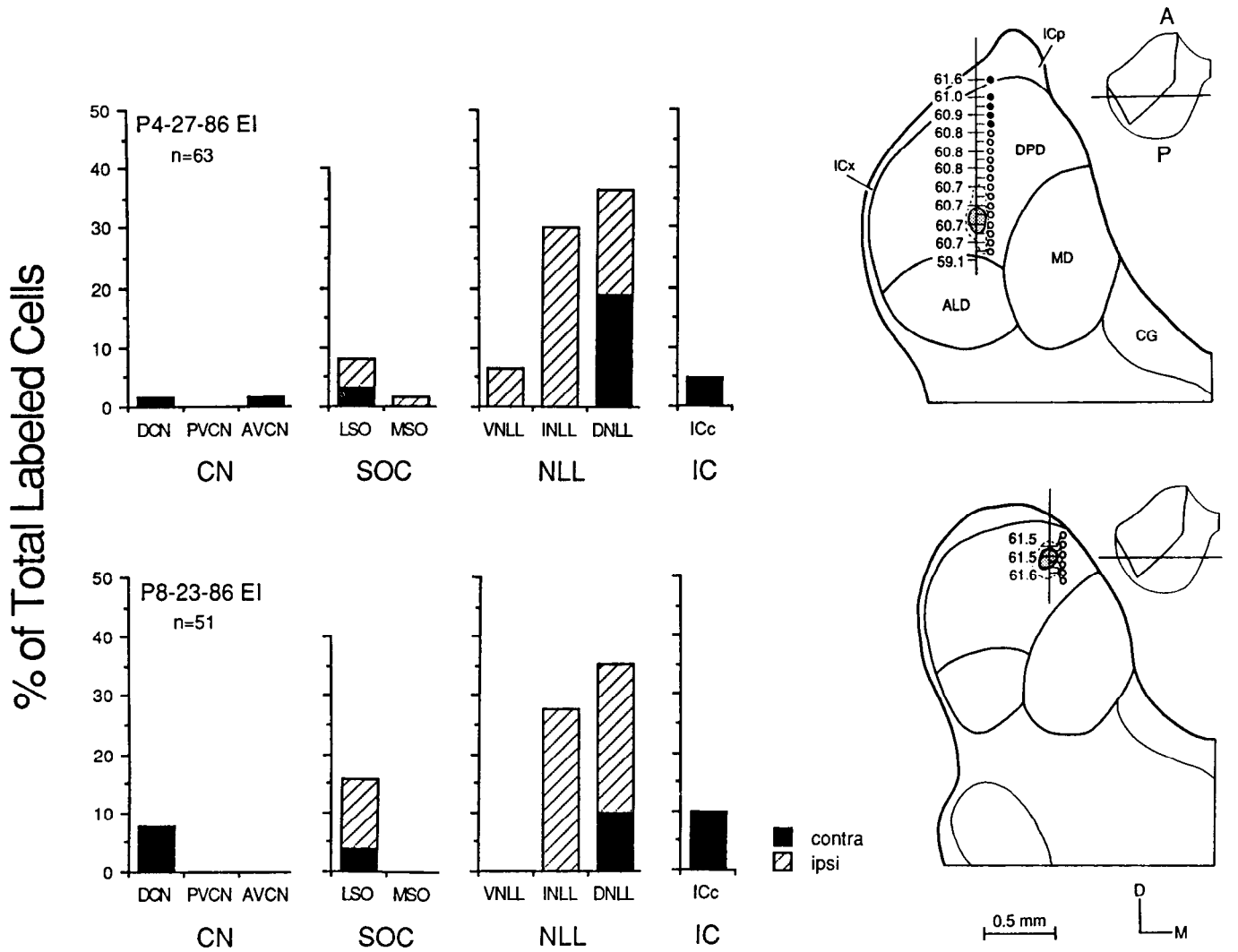

Figure 8. Two cases showing the percentage of labeled cells in the lower auditory nuclei following deposits in the ventromedial EI region of the DPD (see Fig. 5 for explanation). Note the heavy projections from the DNLL, INLL, and LSO. Minor projections were also present from the DCN, VNLL, and contralateral ICc. Symbols: EO neurons, ●; EI neurons, O.

tions of the DPD (Fig. 9, P7-20-87), labeled cells were primarily located in the VNLL and INLL, with fewer cells observed in the MSO or the cochlear nuclei. Thus, it appears that the MSO projects most heavily to the central portion of the EO region and less heavily to the rostral and caudal portions. The VNLL and INLL project throughout the rostrocaudal extent of the DPD. Any difference in the projection pattern from the cochlear nuclei to the DPD is unclear.

Table 2. Percentage of labeled cells in brain-stem auditory nuclei following deposits of HRP in EO regions of the DPD

	Percentage of cells	
Nucleus	Range	Average
DCN	0–10	3
PVCN	0–14	4
AVCN	2–8	5
LSO	0–6	1
MSO	6–35	18
VNLL	17–68	37
INLL	9–20	14
DNLL	0–7	4
ICc	0–17	4

Data represent the range and average percentage for 8 cases.

Discussion

The experiments reported here address the internal organization of the DPD in the mustache bat's IC. The neuronal population of the DPD has an assortment of response characteristics to binaural stimuli that presumably reflect the multitude of functionally distinct projections that this isofrequency region receives (Fuzessery and Pollak, 1985; Wenstrup et al., 1986). By employing both anatomical and physiological techniques, we confirm that neurons exhibiting the major classes of aural properties are topographically segregated into 4 distinct aural regions in the DPD. The chief finding is that each aural region receives a unique set of projections from the constellation of lower auditory nuclei, and thus each DPD region is distinguished both by its neural response properties and by the unique pattern of ascending projections it receives.

A potential confounding is that fibers of passage may have

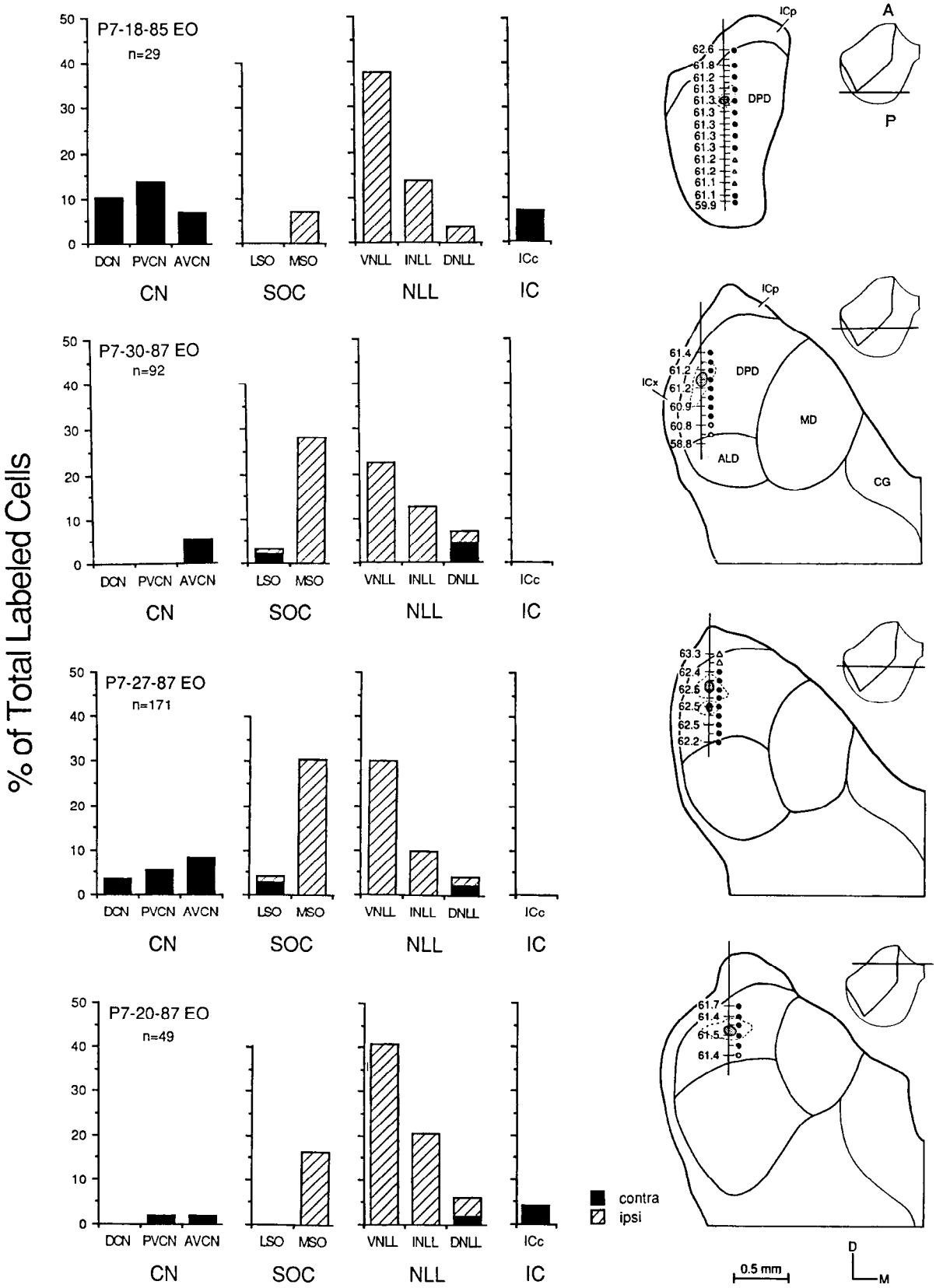

Figure 9. Four cases showing the percentage of labeled cells in the lower auditory nuclei following deposits in the EO region of the DPD. In each case, the deposit was made in a different site along the rostrocaudal axis of the EO region. Explanation as in Figure 5, with cases arranged in a caudal (*top*) to rostral (*bottom*) manner. At caudal sites in the EO region (case P7-18-85), the majority of labeled cells were found in the VNLL, INLL, and the cochlear nuclei. At central positions along the rostrocaudal axis of the EO region (cases P7-30-87 and P7-27-87), fewer cells were found in the cochlear nuclei, and heavy labeling was present in the MSO, VNLL, and INLL. At rostral levels (case P7-20-87), fewer labeled cells were found in the MSO, and heavy labeling was present in the VNLL and INLL. Symbols: EO neurons, ●; EE neurons, △; EI neurons, O.

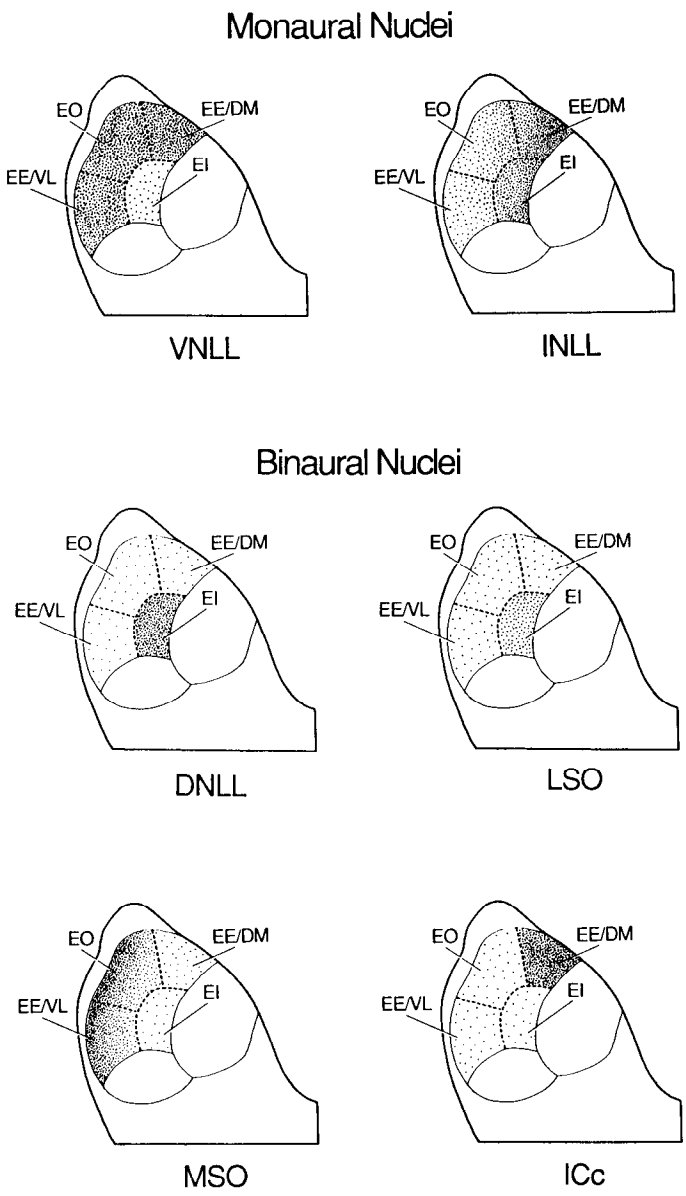

Figure 10. Upper panels, Summary diagram schematically illustrating how monaural auditory nuclei project across the DPD. The data from all cases were pooled to determine whether a particular nucleus projects uniformly across the DPD or whether its projection is more restricted. Regions of *dark shading* indicate the region where the percentage of labeled cells located in a nucleus was highest and where the projections from the nucleus are potentially densest. The VNLL projects heavily to all aural regions of the DPD, except the ventromedial EI region. The INLL projects to all aural regions, but is heaviest in the medial DPD. *Lower panels,* Summary diagram schematically illustrating how binaural nuclei project across the DPD. The DNLL and LSO project to several aural regions but most heavily to ventromedial DPD. In the ventromedial DPD, the projections from the DNLL are heavier than those from the LSO (illustrated by the *denser shading*). The MSO projects primarily to lateral portions of the DPD. The ICc projects heavily to the dorsomedial region of the DPD and sparsely to other aural regions.

been damaged during the advancement of the electrode, thereby labeling cells whose axons did not actually terminate at the injection site. Although we cannot entirely rule out the possibility that such damaged fibers may have contributed to the results, there are reasons for concluding that their contribution was minimal. One reason is that injections in a particular aural region resulted in a similar pattern of labeling among animals. If damaged axons were a major source of HRP uptake, then the same set of axons must have been injured in each case. This situation is unlikely given the differential depths to which the electrodes were advanced among cases and the differences in the positions of the injection sites along the rostrocaudal and/or mediolateral axes (e.g., the 2 injections in the EI region in Figs. 3 and 8). Another reason is that the results we obtained with retrograde transport are in close agreement with anterograde studies, as described below.

Regional projections upon the DPD

The results presented previously show that each aural region of the DPD receives projections from a particular subset of lower nuclei. In this section, we evaluate the projections from the perspective of the lower nuclei; specifically, how the ascending projections of each lower nucleus are distributed within the DPD. We infer the projection pattern of each nucleus on the basis of retrograde transport from large numbers of small deposits covering substantial portions of the DPD, as shown in Figure 10. Before describing these projection patterns, we point out that the best procedure for determining the distribution of projections from lower nuclei would be to inject an anterograde tracer into the 60 kHz region of each nucleus and evaluate how their terminal fields distribute across the DPD. While we did not employ anterograde tracers, anterograde studies of the mustache bat's auditory system have been reported by Zook and Casseday (1985, 1987). The injection sites in the Zook and Casseday studies, however, were made without reference to frequency. In a previous study we determined the loci representing 60 kHz in each lower nucleus (Ross et al., 1988). Therefore, we can identify which of their cases included the 60 kHz regions from their figures showing the locations of the deposit sites within each nucleus. To provide a reliable picture of how projections are distributed within the DPD, we present the projection patterns obtained from the retrograde data of this study and show the close agreement between these patterns and the anterograde results reported by Zook and Casseday (1987).

In general, our findings indicate that the projection fields of monaural nuclei are widespread. As shown in Figure 10, the VNLL projects rather uniformly throughout most of the DPD. The only aural region to which the VNLL does not project is the ventromedial EI region. The INLL also projects throughout the DPD to all 4 aural regions. However, the percentage of labeled cells increased as deposits were made in more medial sites (Fig. 10), indicating that the INLL may project to the entire DPD, but with projections ending most densely in the medial DPD and less densely in the lateral DPD. The other principal monaural nucleus, the cochlear nucleus, rarely contained more than 10% of the labeled cells, making it difficult to quantitatively assess the distribution of the projections from this nucleus.

The injections made in the VNLL by Zook and Casseday (1987, their figure 5A) involved a portion of the 60 kHz representation. The projections were diffusely distributed throughout the DPD but were concentrated dorsally and laterally. This anterograde pattern matches the pattern from the retrograde data shown in Figure 10. Unfortunately, their deposit in the INLL did not include the 60 kHz area.

The retrograde data show that binaural nuclei project to the DPD in a restricted manner. The percentage of labeled cells found in each binaural nucleus was highest when deposits were made in particular aural regions. As shown in Figure 10, the

projections of the DNLL are concentrated within a small portion of the ventromedial DPD, corresponding to the EI region. The highest percentage of labeled cells in the LSO also occurred when deposit sites were in the ventromedial DPD. This implies that both the DNLL and LSO project most densely to the ventromedial EI region. Labeled cells were found in the MSO chiefly with deposits in the lateral DPD, with the percentage of cells increasing as the deposits were made in progressively more lateral sites. The MSO, therefore, projects primarily to the EO and to the ventrolateral EE regions (Fig. 10). The contralateral ICc also projects to the DPD in a restricted manner. As shown in Figure 10, the ICc projects heavily to a limited segment of the rostrocaudal axis of the DPD, from approximately 1200 to 1400 μm, which corresponds to the dorsomedial EE region.

Following deposits of anterograde tracer that included the 60 kHz portions of the medial and lateral superior olives, Zook and Casseday (1987) show labels confined to the ventral and lateral aspects of the DPD. Deposits in the MSO produced labeling concentrated in the lateral DPD (their figure 1B), while deposits in the LSO resulted in label concentrated in the ventromedial DPD (their figure 2). The distribution of anterograde transport from the MSO and LSO is in close agreement with the inferred projection patterns from these nuclei shown in Figure 10. With regard to injections that included the 60 kHz region of the DNLL, they described anterograde projections concentrated in the ventromedial DPD (their figure 6B), which also agrees with the retrograde projection pattern in Figure 10. These results suggest that each lower auditory nucleus has a characteristic pattern of terminations within the DPD that can vary substantially from nucleus to nucleus.

Comparison with studies of the cat's IC

Studies of the cat's ICc also suggest that ascending fibers from the lower nuclei project differentially within isofrequency contours (Roth et al., 1978; Brunso-Bechtold et al., 1981; Henkel and Spangler, 1983; Aitkin and Schuck, 1985; Maffi and Aitkin, 1987). Anatomical studies showed that monaural nuclei, such as the cochlear nucleus and VNLL, project to caudal portions of the ICc, whereas the binaural nuclei of the superior olivary complex project rostrally (Roth et al., 1978; Brunso-Bechtold et al., 1981). These anatomical experiments were done on a large scale, examining the projections to large portions of the ICc rather than to single isofrequency contours. Brunso-Bechtold et al. (1981) used the term nucleotopy to describe the segregation of auditory projections to the ICc with respect to the nucleus of origin. Physiological studies of the cat's ICc showed that neurons having monaural or various binaural properties are grouped within isofrequency contours (Roth et al., 1978; Semple and Aitkin, 1979). Of importance, the nucleotopic projection pattern found in connectional studies correlates strongly with the grouping of aural properties along contours observed in physiological studies. These findings suggest that the aural properties in the ICc are largely a consequence of a differential projection pattern along a contour, a hypothesis corroborated by the results of this study from the mustache bat's DPD.

A different, more detailed view of projections to isofrequency contours is obtained from studies that utilized anterograde tracers injected into one or more lower brain-stem nuclei. The labeling in the ICc resulting from such injections forms dense finger-like bands oriented along axes that closely parallel the fibrodendritic laminae that characterize isofrequency contours. Presumably, each band represents the projections to an isofrequency contour. In the cat's auditory system, the projections from the DNLL, the LSO, the MSO, and the cochlear nuclei display this banding pattern in the ICc (Kudo, 1981; Casseday and Covey, 1983; Henkel and Spangler, 1983; Oliver, 1987; Shneiderman and Henkel, 1987). A question of major importance is what regional domains do the various projection bands that originate from different lower nuclei assume within the sheet of cells forming an isofrequency contour? This feature is poorly understood, but assuming the general organization of the DPD applies to other mammals, the results of the present experiment relate to this question. If it were possible to examine the bands from several sources within a single contour, our results suggest that the afferents from binaural nuclei, such as the MSO, LSO, and DNLL, should occupy specified regions. Moreover, the domains of the afferents from the LSO and DNLL should overlap, but should be largely separate from the territory of the MSO. The projections from VNLL, which is also a prominent nucleus in other mammals, should distribute diffusely within the contour. It is noteworthy that anterograde tracers injected in the cat's VNLL do not produce a banding pattern in the ICc (Whitley and Henkel, 1984), suggesting that this nucleus projects diffusely across the entire central nucleus, and thus within any contour as well.

Construction of binaural response properties and some physiological implications

Assuming that the response properties of a neuronal population are shaped by the pattern of afferents it receives, the difference in projection patterns to each of the aural regions in the DPD should relate directly to physiological features of binaural neurons. Thus, each region characterized by a particular set of projections should be functionally distinguishable from other regions that receive a different set of afferents. Most notable are the differences in the projections to the 2 EE regions and the marked gradation of MSO projections within the EO region. We address these features in greater detail below. In addition, the connectional patterns of the binaural regions are so distinct that we can specify where, and generally how, the various binaural properties are initially shaped from the convergence of inputs from the 2 ears.

The following description of how the binaural response properties in the DPD are initially formed assumes that the dominant projections to an aural region exert the most influence upon the region. Such a description, however, must be incomplete for it neglects the influence from other sources, such as minor contributions from other auditory nuclei and the intrinsic connections within the ICc itself. Bearing these limitations in mind, below we identify 3 major strategies for the initial formation of binaural properties in DPD neurons.

The ventrolateral DPD exemplifies the simplest and most straightforward means of constructing binaural properties in collicular neurons. In this case, binaural EE properties are first created in the MSO, a lower nucleus whose neurons are also largely EE (Moushegian et al., 1967; Goldberg and Brown, 1968, 1969; Guinan et al., 1972a, b; Inbody and Feng, 1981). The binaural properties first created in the MSO are then channeled directly to the ventrolateral DPD (Fig. 11, top panel). It should be noted that this EE region also receives projections from the VNLL and INLL although the specific roles of these projections are not clear.

The properties of the dorsomedial EE region are constructed in a way strikingly different from those in the ventrolateral EE

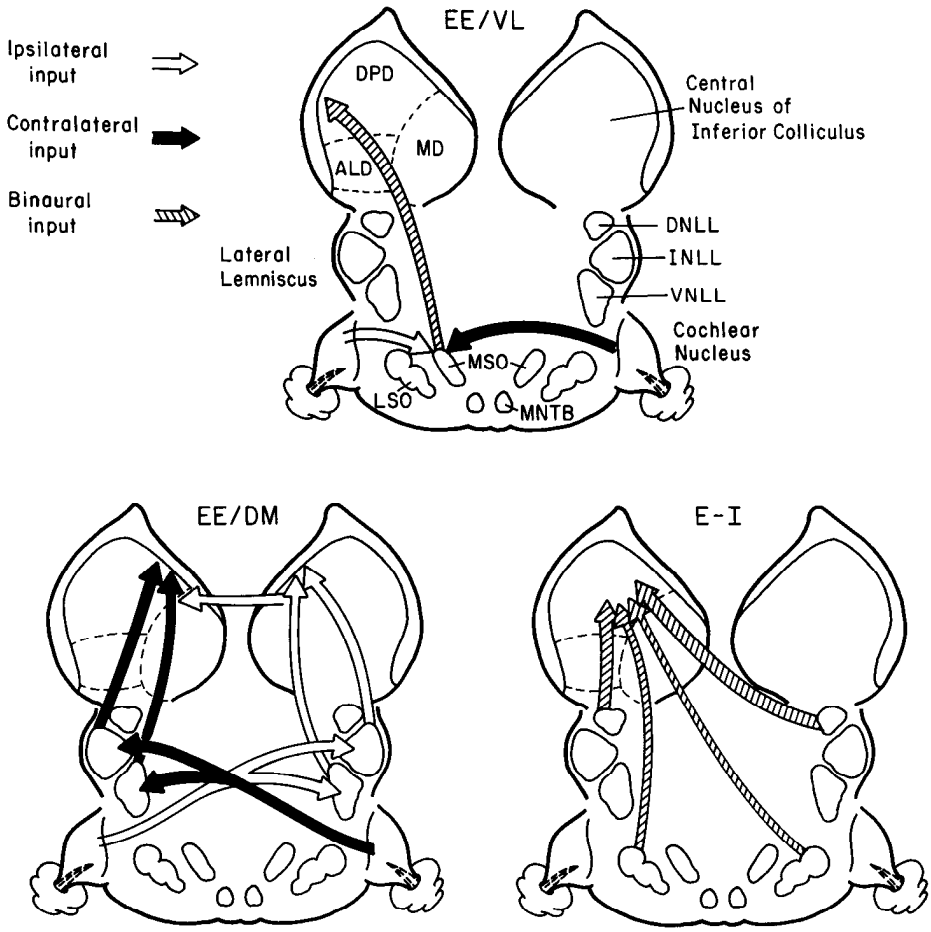

Figure 11. Schematic diagram showing some of the major projections to the ventrolateral EE region (*top panel*) and dorsomedial EE region (*lower left panel*) to illustrate 2 ways that EE response properties are initially formed. Inputs from the ipsilateral ear are shown in *white*, inputs from the contralateral ear are shown in *black*, and projections from binaural nuclei are *striped*. *Lower-right panel* shows projections from binaural nuclei to ventromedial EI region. See text for further explanation.

region discussed above. The primary inputs to the dorsomedial EE region are from 3 sources: the contralateral ICc and the ipsilateral VNLL and INLL, which we assume are monaural in the mustache bat on the basis of connectional studies (Zook and Casseday, 1985, 1987). Based on these inputs, and further assuming the projections are excitatory, the binaural properties of neurons in this region are most likely constructed in the colliculus from the convergence of the monaural inputs from the 2 ears. As shown in Figure 11 (lower-left panel), the contralateral excitation presumably arises via the VNLL and INLL, and the putative ipsilateral excitation arises via the contralateral ICc. Thus, rather than deriving its binaural character directly from a lower brain-stem nucleus with the same aural property, neurons in the dorsomedial EE region are most likely rendered binaural by a convergence of inputs from the 2 ears in the ICc itself.

Despite the fact that aural properties of neurons in both the ventrolateral and dorsomedial DPD fall into the general category of EE, the difference in connections requires that neurons in the 2 regions have different functional properties, perhaps related to their coding of sound location. Several different types of EE neurons have been found in the DPD, each type functionally distinguished by their spatial receptive fields (Fuzessery and Pollak, 1985). Some EE neurons are spatially selective for the midline sound field and thus could play an important role in sound localization (Fuzessery and Pollak, 1985; Fuzessery, 1986). Other EE neurons were much less spatially selective, indicating that these neurons may serve some function other than sound localization that is presently not well defined. Unfortunately, the locations within the DPD of the various types of EE neurons were not determined in the previous studies, and we can say little more about functional distinctions. Studies combining single-unit recordings and localization of recording sites are necessary to discern further distinctions between these 2 regions.

A third way for constructing binaural properties is illustrated by the EI responses of the ventromedial region of the DPD (Fig. 11, lower-right panel). In this case, the excitatory–inhibitory features are presumably formed initially in the superior olive (Boudreau and Tsuchitani, 1968; Goldberg and Brown, 1969; Guinan et al., 1972a; Tsuchitani, 1977) and are channeled to the ICc in 2 ways. The first is a sparse but direct projection from the LSO bilaterally to the ICc. The second is a much larger projection through an intermediary nucleus, the DNLL, which receives direct projections from the LSO and the MSO (Glendenning et al., 1981; Zook and Casseday, 1987).

The finding that the LSO projects only sparsely to the EI region was unexpected. The reason why this result was not expected is that the LSO is a binaural nucleus whose neurons are almost exclusively EI and, in other animals, are tuned predominately to high frequencies (Boudreau and Tsuchitani, 1968; Goldberg and Brown, 1969; Guinan et al., 1972a; Tsuchitani, 1977). Consequently, our original expectation was that there would be a heavy direct projection from the LSO to the EI region of the DPD. A previous study (Ross et al., 1988), however, showed that the LSO projects only sparsely to the DPD, and the present study shows that its projection is regionally segregated to the ventromedial DPD. These results suggest that

the most prominent direct influence of the LSO is on the DNLL and that the LSO exerts its influence on the DPD to a large degree indirectly, via a heavy projection from DNLL to the EI region of the DPD.

The variety of inputs to the ventromedial DPD is consistent with the diversity of EI response properties observed in studies of single units recorded from this area (Wenstrup et al., 1988a). Two features of particular importance are that (1) EI neurons in this region differ in their sensitivities for interaural intensity disparities, and (2) they are arranged in an orderly fashion according to their intensity disparity sensitivity (Fuzessery and Pollak, 1985; Wenstrup et al., 1985, 1986). The arrangement is important because interaural intensity disparities are the major cues animals use to localize high-frequency signals. The subset of EI neurons discharging in response to a sound codes for the particular intensity disparity at the ears and thus for the location of the sound along the horizontal plane (Fuzessery and Pollak, 1985; Pollak et al., 1986; Wenstrup et al., 1986, 1988b). What is not clear is the role this complex circuitry plays in shaping the sensitivities for intensity disparities or its role in establishing an orderly arrangement of EI neurons according to their sensitivity for intensity disparities. Clarifying these issues represents a major challenge for the future.

Physiological implications of projections to the monaural region

The EO region represents a large portion of the DPD that is characterized by the varied and nonuniform set of projections it receives. The variation in the afferent projections suggests that the EO region could be further divided into caudal, central, and rostral subregions. In the caudal EO region, the predominant inputs arise from monaural brain-stem nuclei, such as the cochlear nucleus, the VNLL, and the INLL. Sparse projections originate from the MSO. Likewise, the predominant inputs to rostral EO region are also from monaural nuclei, the VNLL and INLL, with a somewhat heavier projection from the MSO than in the caudal EO region. The portions of the DPD midway along the rostrocaudal axis, however, receive a heavy projection from the MSO, with additional inputs from the VNLL and INLL.

The projections from the MSO to regions of the DPD that have monaural response properties, especially to the EO area midway along the rostrocaudal axis, is one of the most surprising findings of this study. In view of the paucity of information about the more subtle response features of single neurons in this region, or even of the response properties of MSO neurons, the question of what influence the MSO projection exerts on the response properties of neurons in the dorsal DPD is not easy to answer. Nevertheless, several explanations come to mind, and we discuss 3 of these below.

The first explanation is that the MSO neurons projecting to this region are themselves monaural and thus originate from a different population of MSO neurons from those projecting to the dorsolateral EE region. Monaural neurons have been reported in the MSO (Goldberg and Brown, 1968; Harnischfeger et al., 1985), but the evidence for such cells is meager. Although the possibility of a monaural input from the MSO cannot entirely be ruled out, it seems unlikely and there are stronger arguments for alternative explanations. The second possibility is that the DPD neurons in the central portion of the EO region are EO/F neurons and thus are actually binaural. Neurons of EO/F type have been recorded in the DPD (Fuzessery and Pollak, 1985). They are excited by stimulation to the contralateral ear and are unaffected by sounds presented only to the ipsilateral ear. Their defining feature is a facilitated response when stimuli are presented simultaneously to both ears. We raise the possibility that, while such facilitation is apparent in the discharge rates of single units, it was not discernible in the multiunit activity that we monitored to assess aural properties. The third possibility is that the neurons are indeed binaural, but that the stimuli we employed were inadequate to elicit the expression of the binaural input. For example, one important binaural phenomenon is a masking level difference, better known as the cocktail party effect. Psychophysical studies have shown that when a signal is first masked monaurally (the signal and masking noise are presented to the same ear), it can be detected again if the masking noise is simultaneously presented to the other ear (Jeffress, 1972; McFadden, 1975). Thus, a clear improvement in detection or recognition of sounds occurs under appropriate binaural masking conditions. Units exhibiting features appropriate for producing masking level differences have been recorded from the IC of the big brown bat (Schlegel and Singh, 1983), although the binaural properties of these neurons were readily discernible. Their findings also indicate that neuronal responsiveness to complex binaural stimuli may be common in the IC. Here, we suggest the possibility that some DPD neurons that display monaural properties when tested with tones delivered to the 2 ears may require more complex binaural stimuli of the sort employed to demonstrate masking level differences for the influence of the MSO projection, and hence their binaural properties, to be manifest.

In conclusion, we have pointed out that the unique set of projections terminating in each aural region of the DPD suggests that the neurons in each region should have substantially different properties, even when neurons in different regions are of the same general aural type. Moreover, the elucidation of the micro-organization of the DPD provides insights into how the various response properties are created by the convergence of inputs from particular subsets of lower auditory nuclei. Of particular importance is that the set of connections each aural region receives also provides insights into the nature of the functional differences among DPD regions. These insights provide directions for future studies since they suggest which response features should be investigated, as well as the types of stimuli that should be employed.

References

Adams, J. C. (1979) Ascending projections to the inferior colliculus. J. Comp. Neurol. *183:* 519–538.

Adams, J. C. (1981) Heavy metal intensification of DAB-based HRP reaction product. J. Histochem. Cytochem. *3:* 265–274.

Aitkin, L. M. (1976) Tonotopic organization at higher levels of the auditory pathway. Int. Rev. Physiol. Neurophysiol. *10:* 249–279.

Aitkin, L. M. (1985) *The Auditory Midbrain: Structure and Function in the Central Auditory Pathway,* Humana, Clifton, NJ.

Aitkin, L. M., and D. Schuck (1985) Low frequency neurons in the lateral central nucleus of the cat inferior colliculus receive their input predominantly from the medial superior olive. Hear. Res. *17:* 89–93.

Boudreau, J. C., and C. Tsuchitani (1968) Binaural interaction in the cat superior olive S-segment. J. Neurophysiol. *31:* 442–454.

Brunso-Bechtold, J. K., G. C. Thompson, and R. B. Masterton (1981) HRP study of the organization of auditory afferents ascending to the central nucleus of the inferior colliculus in the cat. J. Comp. Neurol. *97:* 705–722.

Casseday, J. H., and E. Covey (1983) Laminar projections to the inferior colliculus as seen from injections of wheat-germ agglutinin horseradish peroxidase in the superior olivary complex of the cat. Soc. Neurosci. Abstr. *9:* 766.

FitzPatrick, K. A. (1975) Cellular architecture and topographic organization of the inferior colliculus of the squirrel monkey. J. Comp. Neurol. *164:* 185–208.

Fuzessery, Z. M. (1986) Speculations on the role of frequency in sound localization. Brain Behav. Evol. *28:* 95–108.

Fuzessery, Z. M., and G. D. Pollak (1985) Determinants of sound location selectivity in the bat inferior colliculus: A combined dichotic and free-field stimulation study. J. Neurophysiol. *54:* 757–781.

Glendenning, K. K., J. K. Brunso-Bechtold, G. C. Thompson, and R. B. Masterton (1981) Ascending auditory afferents to the nuclei of the lateral lemniscus. J. Comp. Neurol. *197:* 673–703.

Goldberg, J. M., and P. B. Brown (1968) Functional organization of the dog superior olivary complex: An anatomical and electrophysiological study. J. Neurophysiol. *31:* 639–656.

Goldberg, J. M., and P. B. Brown (1969) Responses of binaural neurons of dog superior olivary complex to dichotic tonal stimuli: Some physiological mechanisms of sound localization. J. Neurophysiol. *32:* 613–636.

Guinan, J. J., Jr., B. E. Norris, and S. S. Guinan (1972a) Single units in superior olivary complex: I. Responses to sounds and classification based on physiological properties. Int. J. Neurosci. *4:* 101–120.

Guinan, J. J., Jr., B. E. Norris, and S. S. Guinan (1972b) Single units in superior olivary complex. II. Locations of unit categories and tonotopic organization. Int. J. Neurosci. *4:* 147–166.

Harnischfeger, G., G. Neuweiler, and P. Schlegel (1985) Interaural time and intensity coding in the superior olivary complex and inferior colliculus of the echolocating bat, *Molossus ater.* J. Neurophysiol. *53:* 89–109.

Henkel, C. K., and K. M. Spangler (1983) Organization of efferent projections of the medial superior olivary nucleus in the cat as revealed by HRP and autoradiographic tracing methods. J. Comp. Neurol. *221:* 416–428.

Inbody, S. B., and A. S. Feng (1981) Binaural response characteristics of single neurons in the medial superior olivary nucleus of the albino rat. Brain Res. *210:* 361–366.

Irvine, D. R. F. (1986) *Progress in Sensory Physiology, Vol. 7, The Auditory Brainstem,* H. Autrum and D. Ottoson, eds., Springer-Verlag, Berlin.

Jeffress, L. A. (1972) Binaural signal detection: Vector theory. In *Foundation of Modern Auditory Theory,* Vol. 2, J. V. Tobias, ed., pp. 351–368, Academic, New York.

Kudo, M. (1981) Projections of the nuclei of the lateral lemniscus in the cat: An autoradiographic study. Brain Res. *221:* 57–69.

Maffi, C. L., and L. M. Aitkin (1987) Differential projections to regions of the inferior colliculus of the cat responsive to high frequency sounds. Hearing Res. *26:* 211–219.

McFadden, D. (1975) Masking and the binaural system. In *The Nervous System,* Vol. 3, D. B. Tower, ed., pp. 137–146, Raven, New York.

Merzenich, M. M., and M. D. Reid (1974) Representation of the cochlea within the inferior colliculus of the cat. Brain Res. *77:* 397–415.

Mesulam, M.-M. (1982) *Tracing Neuronal Connections with Horseradish Peroxidase,* Wiley, New York.

Moushegian, G., A. L. Rupert, and T. L. Langford (1967) Stimulus coding by medial superior olivary neurons. J. Neurophysiol. *30:* 1239–1261.

Oliver, D. L. (1987) Projections to the inferior colliculus from the AVCN in the cat: Possible substrates for binaural interaction. J. Comp. Neurol. *264:* 24–46.

Oliver, D. L., and D. K. Morest (1984) The central nucleus of the inferior colliculus in the cat. J. Comp. Neurol. *222:* 237–264.

Pollak, G. D., and R. D. Bodenhamer (1981) Specialized characteristics of single units in inferior colliculus of mustache bat: Frequency representation, tuning, and discharge patterns. J. Neurophysiol. *46:* 605–619.

Pollak, G. D., and J. H. Casseday (1989) *The Neural Basis of Echolocation in Bats,* Springer-Verlag, New York.

Pollak, G. D., R. D. Bodenhamer, and J. M. Zook (1983) Cochleotopic organization of the mustache bat's inferior colliculus. In *Advances in Vertebrate Neuroethology,* J.-P. Ewert, R. R. Capranica, and D. J. Ingle, eds., pp. 925–935, Plenum, New York.

Pollak, G. D., J. J. Wenstrup, and Z. M. Fuzessery (1986) Auditory processing in the mustache bat's inferior colliculus. Trends Neurosci. *9:* 556–561.

Rockel, A. S., and Jones, E. G. (1973) The neuronal organization of the inferior colliculus of the adult cat. I. The central nucleus. J. Comp. Neurol. *147:* 11–60.

Rose, J. E., R. Galambos, and J. R. Hughes (1959) Microelectrode studies of the cochlear nucleus of the cat. Bull. Johns Hopkins Hosp. *104:* 211–251.

Ross, L. S., G. D. Pollak, and J. M. Zook (1988) Origin of ascending projections to an isofrequency region of the mustache bat's inferior colliculus. J. Comp. Neurol. *270:* 488–505.

Roth, G. L., L. M. Aitkin, R. A. Andersen, and M. M. Merzenich (1978) Some features of the spatial organization of the central nucleus of the inferior colliculus of the cat. J. Comp. Neurol. *182:* 661–680.

Schlegel, P., and S. Singh (1983) Unmasking in neurons of the inferior colliculus of *Eptesicus fuscus s* with binaural stimulation. Hearing Res. *10:* 331–344.

Schweizer, H. (1981) The connections of the inferior colliculus and the organization of the brainstem auditory system in the greater horseshoe bat (*Rhinolophus ferrumequinum*). J. Comp. Neurol. *201:* 25–49.

Semple, M. N., and L. M. Aitkin (1979) Representation of sound frequency and laterality by units in the central nucleus of the cat's inferior colliculus. J. Neurophysiol. *42:* 1626–1639.

Serviere, J., W. R. Webster, and M. B. Calford (1984) Iso-frequency labelling revealed by a combined [^{14}C]-2-deoxyglucose, electrophysiological and horseradish peroxidase study of the inferior colliculus of the cat. J. Comp. Neurol. *228:* 463–477.

Shneiderman, A., and C. K. Henkel (1987) Banding of lateral superior olivary nucleus afferents in the inferior colliculus: A possible substrate for sensory integration. J. Comp. Neurol. *266:* 519–534.

Tsuchitani, C. (1977) Functional organization of lateral cell groups of cat superior olivary complex. J. Neurophysiol. *40:* 296–318.

Tsuchitani, C., and J. C. Boudreau (1966) Single unit analysis of cat superior olive S-segment with tonal stimuli. J. Neurophysiol. *29:* 694–697.

van Noort, J. (1969) *The Structure and Connections of the Inferior Colliculus,* Van Gorcum and Co., Assen.

Warr, W. B. (1982) Parallel ascending pathways from the cochlear nucleus: Neuroanatomical evidence of functional specialization. In *Contributions to Sensory Physiology,* W. D. Neff, ed., pp. 1–38, Academic, New York.

Wenstrup, J. J., L. S. Ross, and G. D. Pollak (1985) A functional organization of binaural responses in the inferior colliculus. Hearing Res. *17:* 191–195.

Wenstrup, J. J., L. S. Ross, and G. D. Pollak (1986) Binaural response organization within a frequency-band representation of the inferior colliculus: Implications for sound localization. J. Neurosci. *6:* 962–973.

Wenstrup, J. J., Z. M. Fuzessery, and G. D. Pollak (1988a) Binaural neurons in the mustache bat's inferior colliculus: Responses of 60 kHz EI units to dichotic sound stimulation. J. Neurophysiol. *60:* 1369–1383.

Wenstrup, J. J., Z. M. Fuzessery, and G. D. Pollak (1988b) Binaural neurons in the mustache bat's inferior colliculus: Determinants of spatial responses among 60 kHz EI units. J. Neurophysiol. *60:* 1384–1404.

Whitley, J. M., and C. K. Henkel (1984) Topographical organization of the inferior colliculus projections and other connections of the ventral nucleus of the lateral lemniscus in the cat. J. Comp. Neurol. *229:* 257–270.

Willard, F. H., and G. F. Martin (1983) The auditory brainstem nuclei and some of their projections to the inferior colliculus in the North American opossum. Neuroscience *10:* 1203–1232.

Zook, J. M., and J. H. Casseday (1982a) Cytoarchitecture of auditory system in lower brainstem of the mustache bat, *Pteronotus parnellii.* J. Comp. Neurol. *207:* 1–13.

Zook, J. M., and J. H. Casseday (1982b) Origin of ascending projections to inferior colliculus in the mustache bat, *Pteronotus parnellii.* J. Comp. Neurol. *207:* 14–28.

Zook, J. M., and J. H. Casseday (1985) Projections from the cochlear nuclei in the mustache bat, *Pteronotus parnellii.* J. Comp. Neurol. *237:* 307–324.

Zook, J. M., and J. H. Casseday (1987) Convergence of ascending pathways at the inferior colliculus of the mustache bat, *Pteronotus parnellii.* J. Comp. Neurol. *261:* 347–361.

Zook, J. M., J. A. Winer, G. D. Pollak, and R. D. Bodenhamer (1985) Topology of the central nucleus of the mustache bat's inferior colliculus: Correlation of single unit properties and neuronal architecture. J. Comp. Neurol. *231:* 530–546.